

Phosphorus donors in highly strained silicon

Hans Huebl,* Andre R. Stegner, Martin Stutzmann, and Martin S. Brandt

Walter Schottky Institut, Technische Universität München,

Am Coulombwall 3, 85748 Garching, Germany

Guenther Vogg and Frank Bensch

Fraunhofer Institut für Zuverlässigkeit und Mikrointegration IZM,

Institutsteil München, Hansastrasse 27d, 80686 München, Germany

Eva Rauls

Aarhus Universitet, Institut for Fysik og Astronomi,

Ny Munkegade, Bygn. 1520, 8000 Aarhus C, Denmark

Uwe Gerstmann

Institut de Minéralogie et de Physique des Milieux Condensés,

Université Pierre et Marie Curie, Campus Boucicaut,

140 rue de Lourmel, 75015 Paris, France

(Dated: February 6, 2008)

Abstract

The hyperfine interaction of phosphorus donors in fully strained Si thin films grown on virtual $\text{Si}_{1-x}\text{Ge}_x$ substrates with $x \leq 0.3$ is determined via electrically detected magnetic resonance. For highly strained epilayers, hyperfine interactions as low as 0.8 mT are observed, significantly below the limit predicted by valley repopulation. Within a Green's function approach, density functional theory (DFT) shows that the additional reduction is caused by the volume increase of the unit cell and a local relaxation of the Si ligands of the P donor.

PACS numbers: 71.55.Cn, 03.67.Lx, 76.30.-v, 83.85.St

Keywords: hyperfine interaction, strain, DFT, silicon, phosphorus, SiGe, Si, quantum computing

*corresponding author huebl@wsi.tum.de

At present, several approaches for solid-state based quantum computing hardware are actively pursued. The possible integration with existing microelectronics and the long decoherence times [1, 2, 3] are particular advantages of concepts [4, 5, 6, 7] using the nuclear or electronic spins of phosphorus donors in group IV semiconductors as qubits. These concepts require gate-controlled exchange coupling between neighbouring donors. However, to control the exchange coupling in semiconductors with an indirect band structure such as Si, the donor atoms have to be positioned with atomic precision [8] due to Kohn-Luttinger oscillations of the donor wavefunction [5, 9, 10]. Under uniaxial compressive strain in [001] direction, two conduction band (CB) minima are lowered in energy, which leads to a suppression of the oscillatory behaviour of the wavefunction for donors located in the (001) lattice plane [9]. The strain will also affect the wavefunction at the position of the donor atom, which can be observed directly via the hyperfine (hf) interaction between the donor electron and its nucleus [9, 11]. In this letter, we experimentally and theoretically study the hf interaction of phosphorus donors in silicon as a function of uniaxial compressive strain in thin layers of Si on virtual SiGe substrates, extending the regime investigated by Wilson and Feher [11] by a factor of 20 to higher strains. We find that the reduction of the hf interaction significantly exceeds the limit predicted so far [5, 9, 11]. By *ab-initio* DFT calculations using a Green's function approach [12], we are able to show that this reduction is caused by the strain-induced lattice distortion, and a relaxation of the Si lattice next to the P atoms. As the nuclear exchange mediated by the overlap of the donor wavefunction scales with the square of the hf interaction, these results have a direct impact on the rate at which two-qubit operations can be performed [4].

The samples under study were prepared by chemical vapor deposition (CVD) on $30\ \Omega\text{cm}$ B-doped Si (001) substrates [13]. Fully strained thin P-doped Si epilayers with $[P] \simeq 1 \times 10^{17}\ \text{cm}^{-3}$ were grown lattice matched on virtual relaxed $\text{Si}_{1-x}\text{Ge}_x$ -substrates optimized for low dislocation densities. These substrates consist of an intrinsic $0.3\ \mu\text{m}$ Si buffer, a variable sequence of $\text{Si}_{1-y}\text{Ge}_y$ buffer layers with stepwise increasing y , and the actual $2\ \mu\text{m}$ thick virtual $\text{Si}_{1-x}\text{Ge}_x$ substrate with Ge-contents $x = 0.07, 0.15, 0.20, 0.25$, and 0.30 . High-resolution X-ray diffraction (HRXRD) on the 004 and 224 reflexes was used to determine the (in- and out-of-plane) lattice constants of the SiGe layers from which the Ge content and degree of relaxation were calculated using a parabolic dependency of x on the relaxed lattice constants [14] and a linear interpolation of the elastic stiffness constants between Si and Ge

[15]. The $\text{Si}_{1-x}\text{Ge}_x$ layer determines the strain of the Si epilayer: The larger lattice constant of SiGe alloys compared to Si leads to biaxial tensile strain, accompanied by a compensating uniaxial compressive strain in growth direction as shown by the inset in Fig. 1. All Si:P epilayers have a thickness of 15 nm, well below the critical thickness of Si on $\text{Si}_{0.7}\text{Ge}_{0.3}$ [16].

Figure 1 shows the corresponding HRXRD reciprocal space-map (RSM) of the 224 reflex for the $\text{Si}_{0.7}\text{Ge}_{0.3}$ sample. The peak arising from the Si wafer is set to match the lattice constant of c-Si (5.4310 Å) [17]. Extending to lower reciprocal lattice units $q_{\parallel}=\sqrt{2}\lambda/a_{\parallel}$ (in plane) and $q_{\perp}=\sqrt{4}\lambda/a_{\perp}$ (out of plane), a set of diffraction peaks arising from the SiGe buffer layers is observed, followed by the peak of the virtual substrate. The slight difference between the observed values and those expected for fully relaxed $\text{Si}_{1-x}\text{Ge}_x$ alloys (black solid line, [14]) indicates a degree of relaxation of 96.4% of the virtual substrate. Additionally, Fig. 1 shows at $q_{\perp}=0.5715$ ($a_{\perp}=5.3912$ Å) and $q_{\parallel}=0.39686$ ($a_{\parallel}=5.4898$ Å) the diffraction by the strained silicon epilayer. The perfect agreement of q_{\parallel} of the Si epilayer and the virtual substrate reflects the fully strained pseudomorphic growth. It is important to note that the compression in growth direction is in accordance with linear elasticity theory. With $C_{11} = 165.6$ GPa and $C_{12} = 63.9$ GPa as the stiffness constants of Si [15], the relation $\epsilon_{\perp}=-2C_{12}/C_{11} \cdot \epsilon_{\parallel}$ between in-plane and out-of-plane strains $\epsilon_{\parallel}=(a_{\parallel}-a_{\text{Si}})/a_{\text{Si}}$ and $\epsilon_{\perp}=(a_{\perp}-a_{\text{Si}})/a_{\text{Si}}$ predicts a value of $a_{\perp}=5.3856$ Å on the $\text{Si}_{0.7}\text{Ge}_{0.3}$ substrate, in reasonably good agreement with a_{\perp} obtained from Fig. 1, taking into account the width of the thin Si layer caused by the small thickness. Hence, the strain values for the different strained Si samples are obtained from the relaxed in-plane lattice constants of the corresponding SiGe buffers using linear elasticity theory.

To observe the the small amount of P donors in the thin strained layer with high sensitivity, we use electrically detected magnetic resonance (EDMR), which monitors spin resonance via the influence of spin selection rules on charge transport processes [18, 19, 20]. The EMDR experiments were performed in a dielectric ring microwave resonator using a HP83640A microwave source and measuring the spin-dependent photoconductivity at $T = 5$ K in a liquid He flow cryostat under illumination with white light from a tungsten lamp. Resonant changes $\Delta I/I \approx 10^{-5}$ of the photocurrent I were detected using a current amplifier, lock-in detection and magnetic field modulation with 0.2 mT at 1.124 kHz. All spectra were obtained using a microwave power of 50 mW and are normalized to a microwave frequency of 9.749 GHz.

Figure 2 shows the EMDR signal observed as a function of the applied magnetic field

for different angles between the [001] direction of the Si epilayer and the externally applied magnetic field \vec{B}_0 (rotation around [110]). To extract the spectroscopic information, the spectra were fitted with Lorentzian lines. In the range of $B_0 = 346.5$ to 348 mT, anisotropic lines due to the P_{b0} center at the Si/SiO₂ interface are observed with their characteristic anisotropy [21, 22] (dashed lines in Fig. 2). Within the resolution of our experiment, these resonances remain unchanged in the strained layers. The dominant central line with $g = 1.9994$ in the unstrained sample becomes slightly anisotropic under strain and could be assigned to CB electrons [23]. In the unstrained Si layer (cf. Fig. 2 (a)), also the characteristic two hf-split lines of P in Si with a separation of $A_{HF} = 4.2$ mT are easily resolved. The hf lines are isotropic as indicated by the black vertical lines with a center of gravity at $g=1.9985$, well known for unstrained c-Si [23, 24].

In contrast, the hf-split resonances become anisotropic for a strained epilayer as indicated by the black lines in Fig. 2 (b) and (c). For Si on a Si_{0.93}Ge_{0.07} substrate ($\epsilon_{\perp}=-0.00199$), they can be described with an isotropic hf interaction of 1.97 mT and an anisotropic g -factor which varies by $\Delta g=(1.46 \pm 0.1) \times 10^{-3}$ from $\vec{B}_0 \parallel [1\bar{1}0]$ to $\vec{B}_0 \parallel [001]$. Figure 2 (c) shows the results for the epilayer with $\epsilon_{\perp}=-0.00729$ obtained on a Si_{0.75}Ge_{0.25} substrate. Here, the isotropic hf splitting decreases to 0.94 mT, while $\Delta g=(1.21 \pm 0.06) \times 10^{-3}$. The small P-related hf splittings exclude significant segregation of P into the SiGe layers during the growth process, which would lead to larger splittings [25, 26].

For an isolated P donor atom in unstrained Si, the isotropic Fermi-contact hf interaction A_{HF} is given by $8/3\mu_B\pi|\psi(0)|^2$ [11, 27], where μ_B is Bohr's magneton and $|\psi(0)|^2$ is the probability amplitude of the unpaired electron wave function at the nucleus, giving rise to the doublet of hf lines separated by $A_{HF} = 4.2$ mT in Fig. 2(a). To determine $|\psi(0)|^2$, we first note that the cubic crystal field leads to the formation of a singlet ground state plus a doublet and a triplet of excited states instead of a six-fold degenerate ground state of the donor in Si. Only the fully symmetric singlet ground state has a non-vanishing probability amplitude at the nucleus, so that ψ can be written as a superposition $\psi = \sum_{i=1}^6 (1/\sqrt{6})\Phi_i$ of the six valleys contributing to the donor. Here, each Φ_i is a product of the corresponding CB Bloch wavefunction and a hydrogenic envelope-function. The probability of the unpaired electron at the nucleus $|\psi(0)|^2$ becomes $1/6|\sum_{j=1}^6 \Phi_i(0)|^2=6|\Phi(0)|^2$, since due to symmetry $\Phi_i(0)=\Phi(0)$ for all i . Assuming that the only effect of strain is the change of relative population of the CB minima, we similarly find $\psi=\sum_{i=1}^2 (1/\sqrt{2})\Phi_i$ and $|\psi(0)|^2=2|\Phi(0)|^2$

under high uniaxial strain, when only two CB minima contribute. Therefore, in the fully strained case, the hf interaction should be $1/3$ of the unstrained case. In contrast, in Fig. 2 we already observe a reduction to $0.21 \cdot A_{\text{HF}}$, clearly below the $0.33 \cdot A_{\text{HF}}$ limit obtained above. Based on group and linear elasticity theory, Wilson and Feher [11] have evaluated the analytical dependence of $A_{\text{HF}}(\chi)$ on the so-called valley strain $\chi = -\frac{\Xi_u}{3\Delta_c} \left(1 + \frac{2C_{12}}{C_{11}}\right) \epsilon_{\parallel}$, where $\Xi_u = 8.6$ eV [28] is the uniaxial deformation potential, and $6\Delta_c = 2.16$ meV [29] is the energy splitting of the singlet and doublet state in the unstrained material. In Fig. 3, a comparison of the prediction of Eq. (2) in Ref. [11] (dashed line) with the hf splittings determined experimentally (full circles) clearly shows, that pure valley repopulation is not able to describe the experimental data for $x > 0.07$. An empirical treatment of additional radial redistribution effects as discussed in Ref. [30] would lead to $0.30 \cdot A_{\text{HF}}$ for $\chi = -89$ ($x = 1$), only a slight reduction of the repopulation limit and, thus, still at strong variance with the experimental data.

An *ab-initio* calculation of hf interactions is necessary to clarify the situation, but is a demanding task. Already for the unstrained case, the delocalisation of the donor wave function leads to problems in describing the magnetisation distribution correctly [31]. Whereas the energetic position of shallow levels as well as the geometries obtained by usual LSDA supercell calculations can be expected to be in accordance with experimental data, the hf interactions are generally overestimated [12, 32]. Recently, a Green's functions approach (LMTO-GF) has been shown to circumvent this problem of usual supercell approaches [12]. By carefully analyzing the donor-induced resonance at the bottom of the CB, it becomes possible to describe the central-cell correction to effective mass theory by first principles with an accuracy that allows a prediction of superhyperfine interactions for shallow donor states including the Kohn-Luttinger oscillations [12, 33].

In the case of a strained host material, however, the situation becomes more complicated, since excited states are admixed to the former pure singlet ground state. An application of density functional theory (DFT) is only possible in combination with linear elasticity theory: Due to the applied strain, the symmetry of the P donor is reduced, and the resonance at the bottom of the CB is transforming according the a_1 representation in the unstrained case, now shows admixtures of the b_1 and b_2 representations of D_{2d} symmetry. The location of the P donor atom in their nodal planes implies a correlation of these b_1 and b_2 -like orbitals with the admixed doublet state. Since, furthermore, only one component of the diamagnetic

doublet state contributes to the singlet ground state under strain [11], it is reasonable to construct the spin-densities, which enter the self-consistent LSDA total energy calculations for a given valley strain, by $n^\sigma(r) = (1 - \alpha(\chi)) \cdot n_{a1}^\sigma(r) + \alpha(\chi) \cdot n_{b1}^\sigma(r)$, where $\sigma = |\uparrow\rangle$ or $|\downarrow\rangle$. Here, $\alpha(\chi)$ is obtained from the strain-dependent admixture of the doublet states determined by linear elasticity theory (see Eq. (C6) in Ref. [11]). Figure 3 shows that the spin densities constructed this way allow a reasonable description of the pure valley repopulation effect since for an *unrelaxed* structure of an *ideal* Si crystal, the results obtained by Wilson and Feher [11] are nicely reproduced after the self-consistent cycle (cf. open squares in Fig. 3).

We are now able to take into account explicitly *by first principles* the strain of the Si lattice as well as the relaxation around the P donors within. For the optimization of the strained Si cells, we used the efficient self-consistent charge DFT-based tight binding (SCC-DFTB) approach [34]. Optimisation of long slabs (up to 12 unit cells along the [001] direction) show an almost linear dependence of the compression along [001] as an answer to the tensile strain in the (001)-plane, effectively following linear elasticity theory as indicated in the inset of Fig. 3. This result confirms that *linear* elasticity theory remains valid in the complete regime investigated, even up to pure germanium as a substrate ($\chi \approx -89$). The hf parameters calculated with LMTO-GF under these assumptions (cf. open circles in Fig. 3) already become smaller since the donor wavefunction becomes more delocalized as a result of the enhanced volume, exceeding the high-stress limit of $0.33 \cdot A_{\text{HF}}$ obtained above.

This tendency is enhanced, if local relaxation around the P donors is taken into account: According to SCC-DFTB calculations on large, explicitly strained supercells with 512 atoms, this relaxation is dominated by a slight reduction of the bond-length between the P donor and its nearest Si ligands by about 1%, nearly independent of the strength of the tensile strain in the plane of the Si epilayer and already present in the unstrained case. Re-calculating $A_{\text{HF}}(\chi)$ for this geometry with the LMTO-GF code, we find a further reduction (full triangles in Fig. 3). While the theoretically predicted absolute value A_{HF} is ≈ 2 mT too large in the unstrained case without nearest neighbour relaxation, A_{HF} is now in good accordance with the experiment for all χ . The hf interaction observed experimentally in the moderately strained P-doped Si layers can, thus, be explained by the increased volume of the unit cell together with a slight inward relaxation of the nearest Si neighbors. Since already such a small relaxation has a huge influence on the predicted relative hf splittings for the strained material, the remaining discrepancy between experiment and theory

can easily be attributed to uncertainties due to the well-known flatness of the total energy surface in Si [35]. According to our DFT calculation, the decrease of the central P-related hf interaction is accompanied by a remarkable increase of the superhyperfine interaction with neighbouring ^{29}Si atoms. Comparative electron-nuclear double resonance (ENDOR) or electrically detected ENDOR (EDENDOR) [19] measurements could be used to verify these predictions.

Finally, we briefly turn to the anisotropy of the g -factor of the donor. The values observed here are somewhat larger than the values reported by Wilson and Feher [11] and those observed in strained two-dimensional electron gases [36]. Note that a single-valley effect arising from an admixture of the doublet is not expected for uniaxial strain in [001] direction, dominant in our samples. Rather, a pure repopulation effect is expected [11, 37, 38]. However, a detailed calculation of the g -factor under strain including local relaxation appears warranted to understand the origin of the larger Δg observed in our samples.

To summarize, we have presented an experimental and theoretical study of the hyperfine splitting of phosphorus donors in strained layers up to high strain levels of $\epsilon_{\perp} = -0.00882$. The splitting is reduced to values far below predictions published so far. Density functional theory demonstrates that repopulation of the CB minima by strain, the change of the unit cell volume, and a relaxation of the bond length between the P donors and the next nearest Si neighbours are required to account for the observed hyperfine interaction. Our results indicate that there exists no high-stress limit for the reduction of the P-related hf splitting.

This work was supported by the Deutsche Forschungsgemeinschaft (SFB 631).

- [1] J. T. G. Castner, Phys. Rev. Lett. **8**, 13 (1962).
- [2] A. M. Tyryshkin, S. A. Lyon, A. V. Astashkin, and A. M. Raitsimring, Phys. Rev. B **68**, 193207 (2003).
- [3] J. P. Gordon and K. D. Bowers, Phys. Rev. Lett. **1**, 368 (1958).
- [4] B. E. Kane, Nature **393**, 133 (1998).
- [5] B. E. Kane, Fortschr. Phys. **48**, 1023 (2000).
- [6] R. Vrijen, E. Yablonovitch, K. Wang, H. W. Jiang, A. Balandin, V. Roychowdhury, T. Mor, and D. DiVincenzo, Physical Review A **62**, 012306 (2000).

- [7] L. C. L. Hollenberg, A. S. Dzurak, C. Wellard, A. R. Hamilton, D. J. Reilly, G. J. Milburn, and R. G. Clark, Phys. Rev. B **69**, 113301 (2004).
- [8] S. R. Schofield, N. J. Curson, M. Y. Simmons, F. J. Rueß, T. Hallam, L. Oberbeck, and R. G. Clark, Phys. Rev. Lett. **91**, 136104 (2003).
- [9] B. Koiller, X. Hu, and S. Das Sarma, Phys. Rev. B **66**, 115201 (2002).
- [10] C. J. Wellard, L. C. L. Hollenberg, F. Parisoli, L. Kettle, H.-S. Goan, J. A. L. McIntosh, and D. N. Jamieson, Phys. Rev. B **68**, 195209 (2003).
- [11] D. K. Wilson and G. Feher, Phys. Rev. **124**, 1068 (1961).
- [12] H. Overhof and U. Gerstmam, Phys. Rev. Lett. **92**, 087602 (2004).
- [13] S. Kreuzer, F. Bensch, R. Merkel, and G. Vogg, Mat. Sci. Sem. Proc. **8**, 143 (2005).
- [14] J. P. Dismukes, L. Ekstrom, and R. J. Paff, J. Phys. Chem. **68**, 3201 (1964).
- [15] in *Landolt-Börnstein - Group III Condensed Matter* (Springer, 2001), vol. 41 Subvolume A1A.
- [16] S. B. Samavedam, W. J. Taylor, J. M. Grant, J. A. Smith, P. J. Tobin, A. Dip, A. M. Phillips, and R. Liu, J. Vac. Sci. Technol. B **17**, 1424 (1999).
- [17] P. Becker, P. Seyfried, and H. Siegert, Z. Phys. B **48**, 17 (1982).
- [18] J. Schmidt and I. Solomon, Compt. Rend. **263**, 169 (1966).
- [19] B. Stich, S. Greulich-Weber, and J.-M. Spaeth, Appl. Phys. Lett. **68**, 1102 (1996).
- [20] M. S. Brandt, S. T. B. Goennenwein, T. Graf, H. Huebl, S. Lauterbach, and M. Stutzmann, phys. stat. sol. (c) **1**, 2056 (2004).
- [21] E. H. Poindexter, P. J. Caplan, B. E. Deal, and R. R. Razouk, J. Appl. Phys. **52**, 879 (1981).
- [22] A. Stesmans and V. V. Afanas'ev, J. Appl. Phys. **83**, 2449 (1998).
- [23] C. F. Young, E. H. Poindexter, G. J. Gerardi, W. L. Warren, and D. J. Keeble, Phys. Rev. B **55**, 16245 (1997).
- [24] P. R. Cullis and J. R. Marko, Phys. Rev. B **11**, 4184 (1975).
- [25] H. Vollmer and D. Geist, phys. stat. sol. (b) **62**, 367 (1974).
- [26] M. Höhne, U. Juda, J. Wollweber, D. Schultz, J. Donecker, and A. Gerhardt, Mat. Sci. Forum **196-201**, 359 (1995).
- [27] W. Kohn, Solid State Physics **5**, 257 (1957).
- [28] V. J. Tekippe, H. R. Chandrasekhar, P. Fisher, and A. K. Ramdas, Phys. Rev. B **6**, 2348 (1972).
- [29] A. K. Ramdas and S. Rodriguez, Rep. Prog. Phys. **44**, 1297 (1981).

- [30] H. Fritzsche, Phys. Rev. **125**, 1560 (1962).
- [31] E. Hale and R. Mieher, Phys. Rev. **184**, 739 (1969).
- [32] E. Rauls, M. V. B. Pinheiro, S. Greulich-Weber, and U. Gerstmamn, Phys. Rev. B **70**, 085202 (2004).
- [33] W. Kohn and J. Luttinger, Phys. Rev. **98**, 915 (1955).
- [34] T. Frauenheim, G. Seifert, M. Elstner, Z. Hajnal, G. J. D. Porezag, S. Suhai, and R. Scholz, phys. stat. sol. (b) **217**, 41 (2000).
- [35] U. Gerstmamn, E. Rauls, H. Overhof, and T. Frauenheim, Phys. Rev. B **65**, 195201 (2002).
- [36] C. F. O. Graeff, M. S. Brandt, M. Stutzmann, M. Holzmann, G. Abstreiter, and F. Schäffler, Phys. Rev. B **59**, 13242 (1999).
- [37] L. M. Roth, Phys. Rev. **118**, 1534 (1960).
- [38] L. Liu, Phys. Rev. Lett **6**, 683 (1961).

Figures

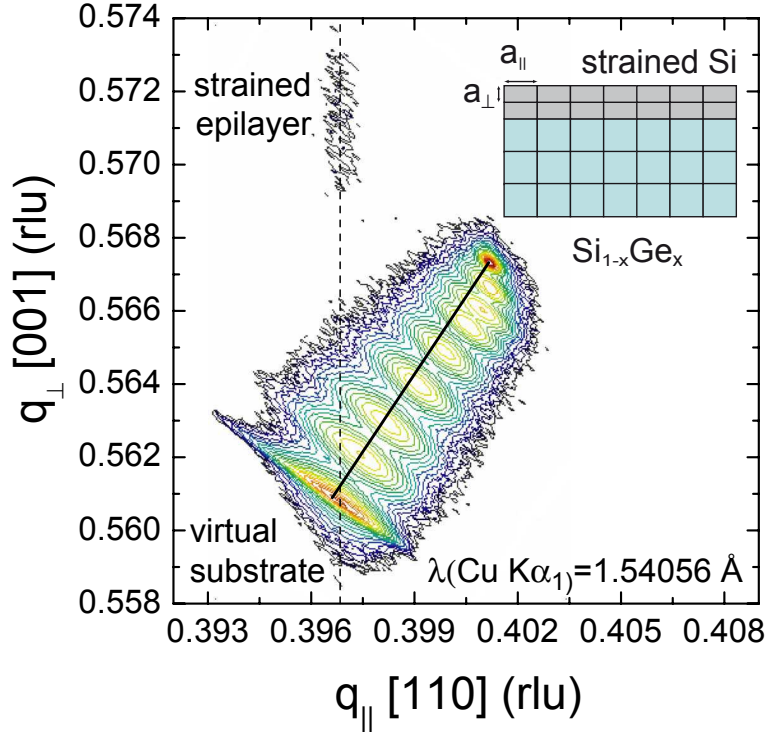


FIG. 1: (color online) Reciprocal space map of the 224 reflex of a 15 nm thick fully strained Si film on a $\text{Si}_{0.7}\text{Ge}_{0.3}$ virtual substrate (log.-scaled iso-intensity plot, Cu $K\alpha_1$ radiation). The straight line represents q_{\parallel} and q_{\perp} predicted for relaxed $\text{Si}_{1-x}\text{Ge}_x$ with $0 \leq x \leq 0.3$ [17].

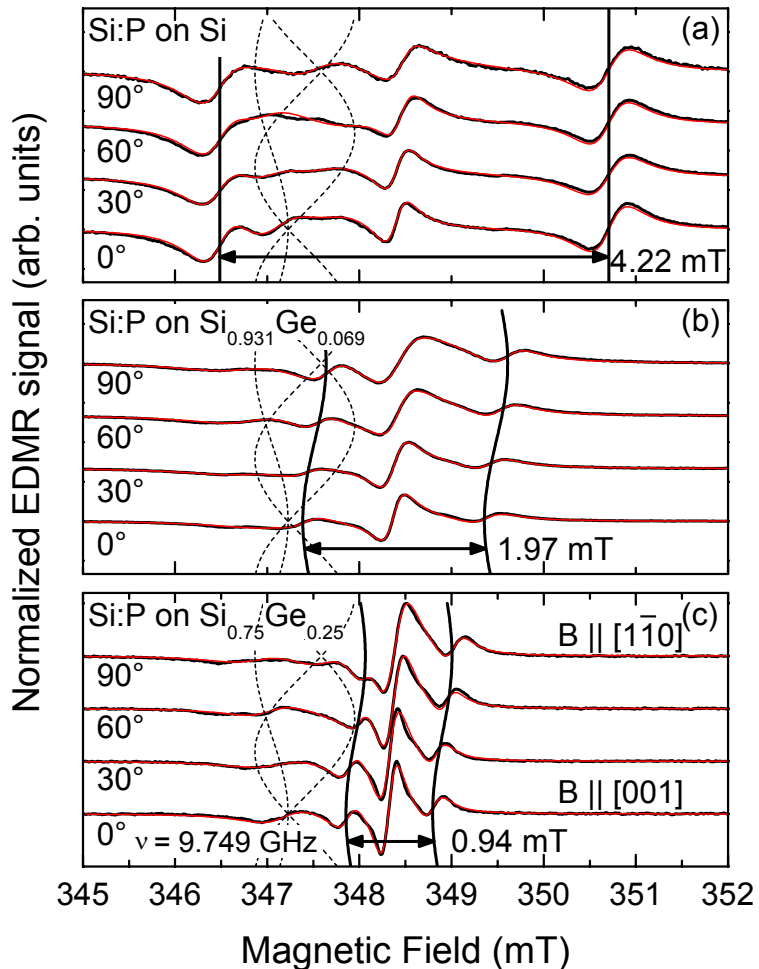


FIG. 2: (color online) Electrically detected magnetic resonance of P donors in relaxed and fully strained Si epilayers on three different $\text{Si}_{1-x}\text{Ge}_x$ virtual substrates as a function of the orientation of the [001] growth direction with respect to the magnetic field \vec{B}_0 for a rotation around [110]. To extract spectroscopic information, the spectra have been fitted using Lorentzian lines. The sum of these lines is shown in red.

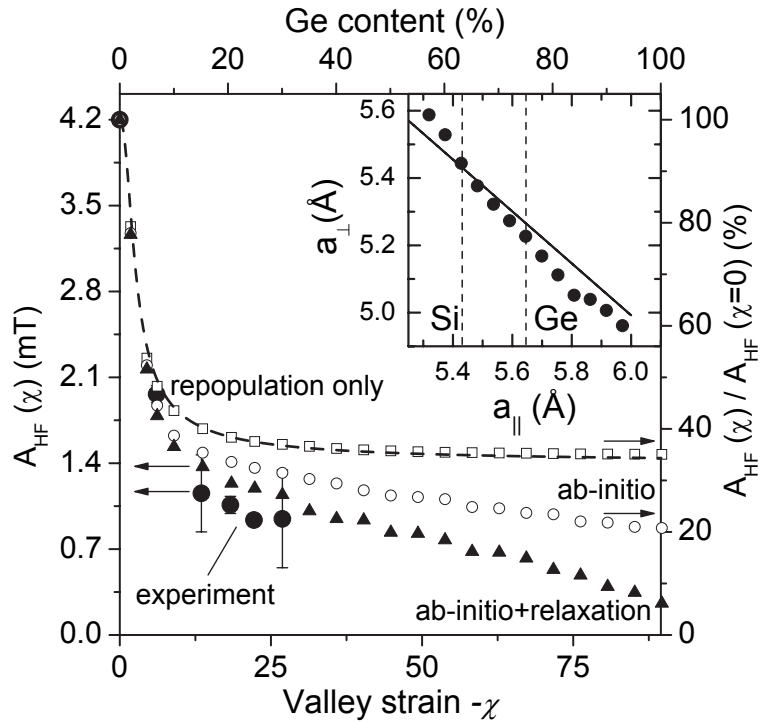


FIG. 3: Hyperfine splittings observed for P in fully strained epilayers on $Si_{1-x}Ge_x$ substrates as a function x and the resulting valley strain. The black dots indicate the experimental data. The dashed line represents the behaviour expected by valley repopulation [11]. The DFT results for valley repopulation only are indicated by open squares, the results including the strain-induced change in the volume of the unit cell by open circles, and those additionally including relaxation of the P nearest neighbors by filled triangles. For the latter and the experimental data the absolute values A_{HF} are shown, the remaining data refers to the relative scale. The insert shows the out-of-plane lattice constant a_{\perp} of thin Si layers (thickness 12 unit cells) as a function of the in-plane lattice constant a_{\parallel} predicted by SCC-DFTB compared to linear elasticity theory indicated by the straight line. Pseudomorphic Si layers on pure Si and Ge substrates are shown by dashed lines.